

Smart Agent-Based Direct Load Control of Air Conditioner Populations in Demand Side Management

Pegah Yazdkhasti*, Julian Luciano Cárdenas–Barrera, Chris Diduch

Department of Electrical & Computer Engineering, Smart Grid Research Center, University of New Brunswick, Fredericton, Canada

ARTICLE INFO

Article history:

Received: 10 November, 2023

Revised: 12 January, 2024

Accepted: 12 January, 2024

Online: 06 February, 2024

Keywords:

Demand-Side Management

Smart Grid

System Identification

Direct Load Control

Load Forecast

Rebound Effect

ABSTRACT

The integration of fluctuating renewable resources such as wind and solar into existing power systems poses challenges to grid reliability and the seamless incorporation of these resources. To address the inherent variability in renewable generation, direct load control emerges as a promising method for demand-side management. Thermostatically controlled appliances, like air conditioners, hold a significant role in this approach. However, effective direct load control necessitates accurate load magnitude estimation and the potential for load shifting. In this paper, we introduce a smart-agent architecture that employs a mathematical model to forecast aggregated power consumption behavior, even when changes are introduced by the controller. To assess system performance, a numerical simulator was developed, demonstrating the system's adaptability to changes, its self-retraining capability, and its continuous improvement in predicting aggregated power consumption.

1. Introduction

This paper builds upon the research initially introduced at ICCAD-2023 [1], where the authors presented a smart agent to make a mathematical model for a population of air conditioners and forecast their power consumption and control it. This paper expands the mathematical formulation for modeling and provides justification for the linear approximation. Additionally, it improves the forecasting model by introducing a new formulation for reserve capacity to reshape the aggregated power demands.

The utilization of clean resources, such as wind and solar power, for electricity generation has experienced substantial growth in the past decade [2]. However, the integration of renewable resources poses challenges to existing power grids, primarily due to the rapid fluctuations in generation, diminishing the reliability and quality of electric power systems [3]. While energy storage devices like batteries can mitigate the swift fluctuations of wind and solar power [4], the cost of deploying renewable energy increases with the use of energy storage. Direct Load Control (DLC) emerges as a cost-effective demand-side management (DSM) method to address the intermittency of generation [5]. Recent studies demonstrate that adjusting set points or operation times of thermostatically controlled loads (TCL), such as electric water heaters or air conditioners, effectively controls aggregated power consumption [6, 7, 8, 9].

The system operator plays a crucial role in balancing generation and demand sides, and an accurate forecast of the power consumption is essential for this task. In a DLC program, the system operator needs to understand the controller's capacity to increase or decrease the load, providing feasible instructions.. This research focuses on developing a methodology for fast and accurate load controllability forecasting.

In recent years, significant efforts have been dedicated to developing mathematical models and control strategies aimed at effectively managing the aggregate demand of air conditioners. One approach involves designing a control strategy to adjust the thermostat set point, thereby reducing peak demand and alleviating the impact of renewable energy variability [10, 11]. Alternatively, centralized or distributed/decentralized control strategies have been explored, focusing on directly managing the on/off states of AC compressors [11, 12, 13, 14, 15]. However, these methods fall short in providing practical means to estimate essential model parameters like thermal capacitance/resistance, or to dynamically adapt the model to changing conditions. Another challenge lies in the absence of information regarding the capacity to increase or decrease the total load within a future time window.

In response to these challenges, several studies have shifted focus towards forecasting the controllable load. Some utilize neural networks to predict air conditioning power consumption

*Corresponding Author: Department of Electrical & Computer Engineering, Smart Grid Research Center, University of New Brunswick, Fredericton, Canada, Email: pegah.ykh@unb.ca

based on temperature, humidity, and historical power consumption [16, 17, 18]. Others employ regression-based algorithms coupled with Kalman filters to forecast air-conditioning load using historical data [19]. Least square support vector machines have also been proposed for short-term load forecasts [20]. However, these methods may face impracticalities when integrated with a control system that alters load behavior. Furthermore, none of these methods offer insights into how much the load can be changed due to a control action or formulate the control capacity.

Introducing a dynamic process and a state space model, our proposed methodology provides an efficient and accurate forecast of the controllable load for the system operator. By constructing a model adaptable to changes in thermal parameters and load behavior, our method surmounts limitations associated with traditional approaches. Furthermore, it equips the system operator with the ability to estimate the controllable capacity of the load, a critical factor in load balancing tasks.

The effectiveness of our methodology was rigorously evaluated through simulations, comparing its performance with existing methods. The results demonstrate that our proposed method surpasses existing approaches in terms of both accuracy and speed. This underscores its potential to offer a more efficient and reliable solution for managing the demand side in response to the integration of renewable resources.

In conclusion, this paper introduces a novel methodology for forecasting the controllable load of air conditioners, capable of adapting to changes in thermal parameters and load behavior. The proposed methodology not only delivers an accurate and efficient load forecast but also empowers the system operator to estimate the controllable capacity of the load. With promising results in simulations, our method holds the potential for practical implementation, promising improved demand side management in response to the integration of renewable resources.

The remainder of this paper is structured as follows: Section 2 provides an overview of the system architecture, while Section 3 offers a concise introduction to the mathematical model of the system. The learning algorithm is detailed in Section 4, and Section 5 outlines the process of generating forecasts. The capacity to control the load is formulated in Section 6. The paper concludes with the presentation of simulation results in Section 7.

2. System Architecture

The objective of this study is to devise a smart agent for the efficient management of power consumption in thermostatically controlled appliances. This system operates within a hierarchical structure, collaborating with a system operator or a virtual power plant (VPP). Its role is to receive a target aggregated power consumption, interact with a load aggregator, and send control signals to adjust the load. The goal is to minimize the discrepancy between the measured and desired power consumption while maintaining customers' comfort. Figure 1 provides an overview of the system, which encompasses a load aggregator with three distinct modules:

1. Learning Model Module: This module is tasked with estimating a mathematical model that articulates the power consumption of the aggregated load based on input parameters.

2. Forecasting Module: Leveraging the estimated mathematical model and input forecasts, this module generates predictions for the baseline load and reserve capacity. Input forecasts encompass variables like weather conditions, occupancy patterns, and other factors influencing power consumption. The baseline load forecast represents the expected power consumption without any control action, while the reserve capacity forecast indicates the potential power reduction or increase through controller actions. These forecasts guide the controller in determining appropriate control signals to align the load with the desired power consumption.
3. Responsible for adhering to the desired aggregated load set by the system operator, this module controls the load. Further details on a simplified implementation of such a controller are presented in [21].

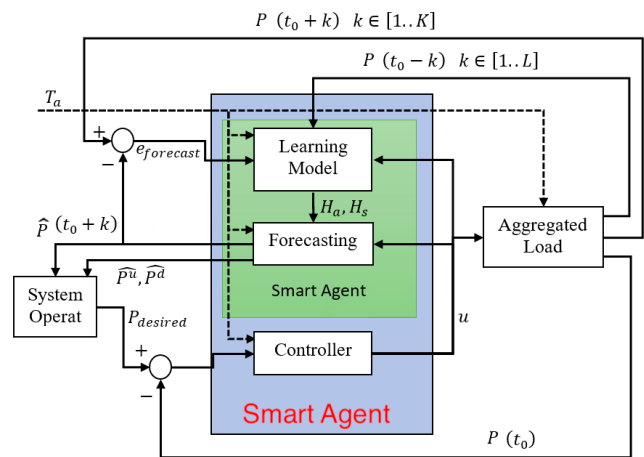


Figure 1: A block diagram for direct load control system [1]

In Figure 1, the power consumption of the load population (Aggregated Load) is input into the load aggregator at the current time denoted by t_0 . Historical data from prior measurements ($P(t_0 - k)$ for times preceding t_0) is utilized by the 'Learning Model' to establish a mathematical model for the system (H_a and H_s). Subsequently, the 'Forecasting' module utilizes this model to generate forecasts for the baseline load and control capacity. In the future, upon obtaining actual measurements of the aggregated load, the forecast error can be calculated as the difference between forecasted and actual power ($e_{forecast}$). This error serves as a trigger mechanism, initiating the training process.

3. Modeling the Aggregated Load

The controllable load in this research are a population of air conditioners. A Mathematical model can provide a powerful tool to analyze the behavior of such system. The following sections will present a commonly used model for single AC and a population of ACs.

3.1. Individual Load

In this context, we denote $m(k)$ as the on/off state of the air conditioner at time k , and T as the room temperature. The dynamics of room temperature changes are governed by Equation (1), a widely adopted formulation in the literature [22, 23, 12, 21]:

$$\dot{T}(t) = -\frac{1}{CR}(T(t) - T_a(t) + m(t)RP_{nom}\eta) \quad (1)$$

Here, R denotes the thermal resistance of the room, C is the thermal capacitance of the room, T_a represents the ambient temperature, P_{nom} corresponds to the nominal power rating of the air conditioner, and η stands for the coefficient of performance. The air conditioner switches on ($m(t) = 1$) when the room temperature surpasses the higher threshold setpoint, aiming to reduce the room temperature until it reaches the lower threshold, at which point the air conditioner turns off ($m(t) = 0$).

3.2. Aggregated Load

The power consumption of an air conditioner (AC) can be conceptualized as a system with two inputs: the thermostat setpoint (as the controllable input) and ambient temperature (as the disturbance signal). Other parameters, such as thermal resistance and capacitance, may be considered as external hidden parameters of the system.

Simulation results demonstrate that the aggregated power demand reaches a steady-state value when the inputs remain constant, as depicted in Figure 2. In general, the steady-state response of the aggregated power demand to the inputs is nonlinear. However, this surface can be approximated by a plane described by:

$$P_{ss}(T_a, T_s) = P_{ss0} + \alpha T_a + \beta T_s, \quad T_a < 34^\circ\text{C}, T_s \leq T_a \quad (2)$$

Figure 2 illustrates the simulated steady-state aggregated power demand vs. the value obtained from (3). As expected, around the nonlinear zone of high ambient temperature, the plane exhibits larger differences than the simulated power demand. However, for the middle sections of the surface, it provides a good approximation for the steady-state aggregated power demand, with the error range over the middle part of the surface being less than 5%.

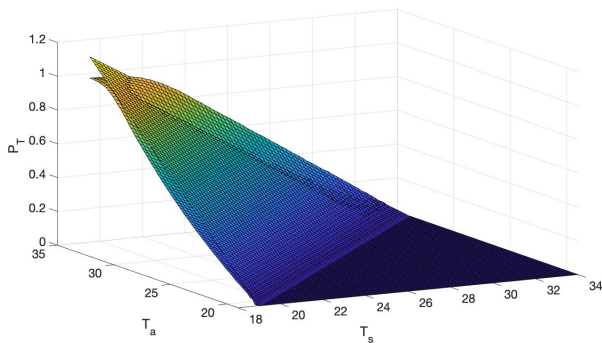


Figure 2: Comparison of the Approximated Plane Surface given by (2) with Simulated Aggregated Power Demand

Through numerical calculations, the coefficients for the best-fitting plane have been determined as:

$$P_{ss}(T_a, T_s) = 0.075T_a - 0.075T_s \quad (3)$$

With this observation, it becomes plausible to consider modeling this system as a Linear Time-Invariant (LTI) system, with the equilibrium point representing the DC gain of the model. Assuming the system is given by:

$$\delta P(s) = H_a(s)\delta T_a(s) + H_s(s)\delta T_s(s) \quad (4)$$

Here, δP denotes changes in the aggregated demand from the equilibrium point due to variations in ambient temperature and thermostat setpoints ($\delta T_a, \delta T_s$). H_a and H_s represent the LTI transfer functions for T_a and T_s respectively. The steady-state output is then given by:

$$\delta P_{ss} = H_a(0)\delta T_a + H_s(0)\delta T_s \quad (5)$$

This equation mirrors (2), where $H_a(0) = \alpha$ and $H_s(0) = \beta$.

Now, by approximating the aggregated demand with a LTI system, the dynamic response of the system can be captured by[24]:

$$P(k) = y_a(k) + y_s(k) + P_0 \quad (6)$$

Here, P_0 denotes the aggregated demand at the equilibrium point (or P_{ss}), while y_a and y_s represent the change in aggregated power consumption with respect to the equilibrium point, caused by variations in the ambient temperature and thermostat set point, respectively. These LTI system can be represented in state space model as:

$$H_a : \begin{cases} x_a(k+1) = A_a x_a(k) + B_a u_a(k), \\ y_a(k) = C_a x_a(k) \end{cases} \quad (7)$$

and

$$H_s : \begin{cases} x_s(k+1) = A_s x_s(k) + B_s u_s(k), \\ y_s(k) = C_s x_s(k) \end{cases} \quad (8)$$

where the matrices A_a, B_a, C_a, A_s, B_s and C_s should be identified through the learning process.

4. Learning Model

The purpose of this module is to formulate an approximation model for the population of air conditioners, eliminating the need for knowledge about any of the physical parameters introduced in Section 3.

The details of the model learning process is presented in [24]. As a short summary, the learning procedure initiates when the forecast error surpasses a predefined threshold level. At this juncture, T_a and T_s are determined, and the controller is temporarily disabled to prevent any artificial fluctuation in the aggregated power consumption.

The learning process encompasses two steps:

1. Determining H_a while holding T_s constant. In this scenario, changes in the output power are solely governed by variations in T_a .
2. Determining H_s when a small change is applied to T_s , and the effect of changes in T_a can be estimated and removed using H_a . The formulations for these steps are elaborated in detail in [24].

5. Load Forecast

To generate a load forecast, one can utilize the forecasted values of the model inputs in equations (7)-(8) to obtain a forecast for the output. However, this requires measurements of the states, which are not physical parameters that can be directly measured. As a result, a state observer is required to estimate these states.

5.1. State Estimation

The overall architecture of the state observer for this system is shown in Figure 3. In the figure, the changes in the output power are denoted by y , while the estimated impact of u_s and u_a are denoted by \hat{y}_s and \hat{y}_a , respectively. The difference between the estimated changes and the actual change in the aggregated power is then fed to the state model through observer gains H_s and H_a to improve state estimation.

$$\begin{cases} \hat{x}_a(k+1) = A_a \hat{x}_a(k) + B_a u_a(k) + H_a C_a (x_a(k) - \hat{x}_a(k)) \\ \hat{y}_a(k) = C_a \hat{x}_a(k) \end{cases} \quad (9)$$

and similarly for the x_s state:

$$\begin{cases} \hat{x}_s(k+1) = A_s \hat{x}_s(k) + B_s u_s(k) + H_s C_s (x_s(k) - \hat{x}_s(k)) \\ \hat{y}_s(k) = C_s \hat{x}_s(k) \end{cases} \quad (10)$$

where \hat{x}_a and \hat{x}_s are the estimated states.

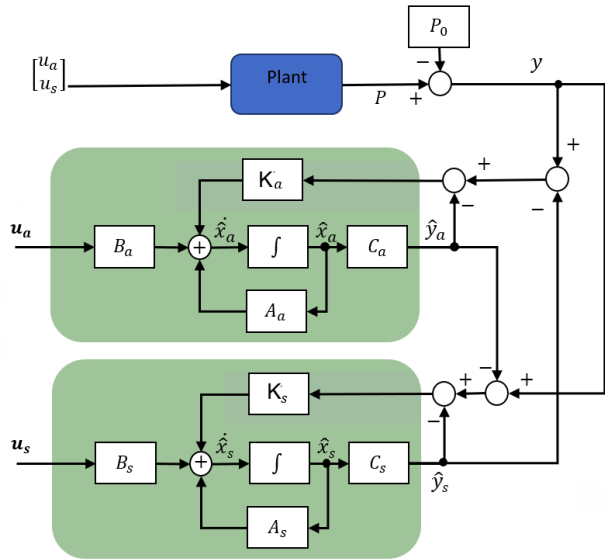


Figure 3: The state observers for each input [1].

These equations can be rewritten in a matrix format as:

$$\begin{cases} \hat{x}(k+1) = \mathcal{A} \hat{x}(k) + \mathcal{B} \begin{bmatrix} u_a \\ u_s \end{bmatrix} + \begin{bmatrix} K_a \\ K_s \end{bmatrix} (y(k) - C \hat{x}(k)) \\ \hat{y}(k) = C \hat{x}(k) \end{cases}$$

where

$$\mathcal{A} = \begin{bmatrix} A_a & 0 \\ 0 & A_s \end{bmatrix}, \quad \mathcal{B} = \begin{bmatrix} B_a & 0 \\ 0 & B_s \end{bmatrix} \quad (11)$$

and

$$C = [C_a \quad C_s] \quad (12)$$

By considering the state error: $\tilde{x}(k) = x(k) - \hat{x}(k)$, we will have:

$$\tilde{x}(k+1) = (\mathcal{A} - KC) \tilde{x}(k) \quad (13)$$

And K can easily be determined so that the dynamics of the state error would be faster than the y system through functions such as pole placement technique in MATLAB.

5.2. Forecasting Baseline Load

When forecasting the baseline load, we operate under the assumption that the controller does not influence the load. Let's consider a forecasting horizon of L samples, assuming that the forecast is generated at time index k_0 . Within this interval, we have:

$$\hat{u}_a(k) = \hat{T}_a(k) - \hat{T}_{a0} \quad k \in [k_0 + 1, k_0 + L] \quad (14)$$

$$\hat{u}_s(k) = 0 \quad k \in [k_0 + 1, k_0 + L] \quad (15)$$

Here, $\hat{T}_a(k)$ is the forecasted ambient temperature at time k . Then the forecast of the baseline aggregated power will be:

$$\hat{P}_b(k) = P_0 + \hat{y}_a(k) \quad k \in [k_0 + 1, k_0 + L] \quad (16)$$

where P_0 is the power consumption at equilibrium point and

$$\begin{cases} \hat{x}_a(k+1) = A_a \hat{x}_a(k) + B_a \hat{u}_a(k) \\ \hat{y}_a(k) = C_a \hat{x}_a(k) \end{cases} \quad (17)$$

where the initial state $\hat{x}_a(k_0)$ can be obtained from the state observer that was presented earlier.

Equation (16) operates under the assumption that no previous control actions have occurred, implying no fluctuations in the aggregated power resulting from prior thermostat changes. Nevertheless, past control actions may continue to influence future power consumption. Given that the forecasting module receives information about each control signal to the thermostat setpoints, it can consistently revise the state space variables of the system. Consequently, the forthcoming changes in \hat{y}_s can be determined by:

$$\begin{cases} \hat{x}_s(k+1) = A_s \hat{x}_s(k) \\ \hat{y}_s(k) = C_s \hat{x}_s(k) \end{cases} \quad (18)$$

and the baseline load will be:

$$\hat{P}_b(k) = \hat{P}_0 + \hat{y}_a(k) + \hat{y}_s(k) \quad k \in [k_0 + 1, k_0 + L] \quad (19)$$

The payback effect, also known as rebound, is a well-established phenomenon in DSM. It characterizes the transient surge in aggregated power that occurs once control over the aggregated load is relinquished, allowing the power to revert to its baseline. This transient, initiated when the system shifts from controlled to uncontrolled operation, has the potential to give rise to unexpected secondary demand peaks.

The controller, tasked with executing demand-side management measures, holds the key to influencing the rebound effect by sustaining control over the devices even beyond the system operator's requested interval. However, this strategy may not always be practical or desirable, particularly if associated with high costs or energy consumption. Hence, in this section, we assume that the controller will exclusively operate during the specified interval, refraining from additional adjustments thereafter.

To equip the system operator with valuable insights into the repercussions of control actions, we introduce a method for estimating the payback of any desired demand even before initiating control. This approach aids the system operator in evaluating the acceptability of control actions and preemptively avoiding an escalation in future peak demands. By furnishing a dependable estimate of the payback effect, this method empowers the system operator to optimize the control strategy and mitigate potential risks to power system operation.

5.3. Approximating Control Signal

Let us consider a scenario where the system operator or VPP issues a dispatch, denoted by $\Delta P_d(k)$, for a control interval of C samples. In this scenario, the desired load can be considered as a change to the baseline load, which is given by:

$$\Delta P_d(k) = P_d(k) - \hat{P}_b(k) \quad (20)$$

Here, $\Delta P_d(k)$ represents the amount of power that needs to be added to or reduced from the baseline load. To effect this change, the thermostat set points, \hat{u}_s , need to be adjusted so that they create appropriate \hat{y}_s values.

Now, the controller needs to generate a $\hat{u}_s(k)$ that results in the output $\hat{y}_s(k)$, matching $\Delta P_d(k)$. This assumes that the linear model remains valid when y_s changes by ΔP_d .

$$\begin{cases} \hat{x}_s(k+1) = A_s \hat{x}_s(k) + B_s \hat{u}_s(k) \\ \hat{y}_s(k) = \Delta P_d(k) = C_s \hat{x}_s(k) \end{cases} \quad (21)$$

This equation can be rewritten as:

$$\Delta P_d(k+1) = C_s [A_s \hat{x}_s(k) + B_s \hat{u}_s(k)] \quad (22)$$

And the control signal, $\hat{u}_s(k)$ will be:

$$C_s B_s \hat{u}_s(k) = \Delta P_d(k+1) - C_s A_s \hat{x}_s(k) \quad (23)$$

If the order of the system model is n , then the matrices C_s and B_s will have dimensions $1 \times n$ and $n \times 1$, respectively. The product $C_s B_s$ will then result in a scalar value, and:

$$\hat{u}_s(k) = (C_s B_s)^{-1} (\Delta P_d(k+1) - C_s A_s \hat{x}_s(k)) \quad (24)$$

subject to:

$$-\alpha \leq u_s(k) \leq \alpha \quad (25)$$

for customers' comfort (will be described more in detail in Section 6). Then, the thermostat set points will be:

$$\hat{T}_s(k) = T_{s0} + \hat{u}_s(k) \quad (26)$$

for k in the control interval. It should be noted that initial state variable, $\hat{x}_s(k_0)$, is estimated using the state observer described in Section 5.1.

Figure 4 illustrates an example of an arbitrary desired aggregated load, represented by the top curve. The baseline load forecast, \hat{P}_b , is also shown in this figure, where the forecast interval is 6 : 00 – 10 : 00 am. The desired aggregated load for the interval of 7 : 00 – 8 : 30 am (control interval) is denoted by P_d . Equations (24)-(26) were utilized to determine how the thermostat set points should be adjusted in order to achieve the desired load. The resulting adjustments are illustrated by the bottom curve of Figure 4.

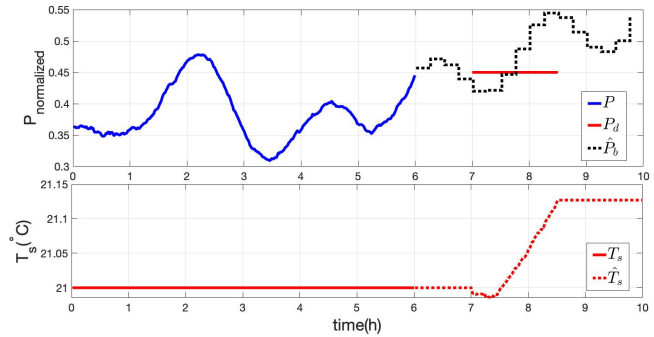


Figure 4: Example of desired load vs. calculated thermostat set point adjustments to follow the load.

5.4. Forecasting Rebound

Once the system operator changes the shape of the power demand over an interval, the profile of the demand will also change in the subsequent intervals, which is referred to as the payback or rebound effect of the control action. If an optimal controller adjusts the thermostat set points to follow the desired load demand and stops controlling it after that interval, the forecasting module can predict the shape of the demand after the control interval even before it starts. This feature can be beneficial for the system operator to estimate the shape of the load after a proposed desired aggregated load and determine if the consequences of the control actions are acceptable (e.g., not producing a larger peak in the future). However, it should be noted that various control strategies may affect this forecast.

Let us assume that the system operator issues a desired aggregated power demand, denoted by $P_d(k)$. This desired load can be considered as a change to the baseline load:

$$P_d(k) = \hat{P}_b(k) + \Delta P_d(k), \quad (27)$$

where $\Delta P_d(k)$ is the amount of power that should be added to or reduced from the baseline load. This change should be achieved by adjusting the thermostat set points (\hat{u}_s) to create an appropriate \hat{y}_s . Thus, the controller should create a $\hat{u}_s(k)$ to match $\hat{y}_s(k)$ with $\Delta P_d(k)$, so an estimation of the control signal will be:

$$\hat{u}_s(k) = (C_s B_s)^{-1} (\Delta P_d(k+1) - C_s A_s \hat{x}_s(k)) \quad (28)$$

Using (28), an estimation of the thermostat control signal can be calculated with the given desired aggregated load. With this

estimated u_s for the control interval and the forecast of the ambient temperature, a new forecast can be generated to approximate the payback of a control action.

$$\begin{cases} \hat{x}_s(k+1) = A_s \hat{x}_s(k) + B_s \hat{u}_s(k) & \text{for } k \text{ in control interval} \\ \hat{x}_s(k+1) = A_s \hat{x}_s(k) & \text{otherwise} \\ \hat{y}_s(k) = C_s \hat{x}_s(k) \end{cases} \quad (29)$$

The aggregated power demand will be:

$$\hat{P}_{\text{payback}}(k) = \hat{P}_0 + \hat{y}_d(k) + \hat{y}_s(k) \quad (30)$$

6. Feasible Desired Demand

One of the key parameters in DLC is ensuring that the controller does not interfere with customers' comfort. For air conditioners, the controller can adjust the thermostat set point to change the aggregated power consumption to follow a desired load. However, if the controller sets the thermostat to a very high or very low value, it may cause discomfort for the end-users and prompt them to opt-out of the DLC program. Therefore, the controller cannot change the thermostat set point to any arbitrary value. The set point must be changed within a certain range to ensure that customers remain comfortable.

This means that the system operator must send a desired demand that can be followed without disturbing the customers. Such a demand is called a feasible desired demand. To ensure that only feasible desired demands are sent, a method will be presented in the next subsections that defines more precisely the customers' comfort and the criteria for feasible desired demands.

6.1. Customers' Comfort

One method of ensuring customers' comfort in DLC is to limit the range of change for the thermostat set point. The preferred thermostat set point for a group of loads can be denoted by T_s^0 . The controller can then adjust the T_s within the range of $[T_s^0 - \alpha, T_s^0 + \alpha]$, where α determines the comfort zone. Once the T_s reaches these limits, the controller cannot adjust it beyond this range, thus losing control over the aggregated power. This signifies the point when there is no more reserve capacity available.

It is crucial to note that this method of limiting the range of T_s affects the controller's ability to adjust the aggregated power consumption to follow a desired load. Infeasible desired loads may arise due to the limitations imposed by the comfort zone. Thus, the system operator should only send feasible desired loads that can be followed without disturbing the customers' comfort. In the following subsections, the concept of customers' comfort and feasible desired loads will be defined more precisely, and a method for informing the system operator about the criteria for feasible desired loads will be presented.

6.2. Formal Formulation

A feasible desired dispatch is a power profile that satisfies three conditions. First, it should be within the range, i.e. $0 \leq P_d(k) \leq P_{\text{max}}$.

Second, the controller should be able to produce appropriate changes to the thermostat set points, so that the aggregated demand of the loads would follow the desired load. Third, the changes on the thermostat set points should not exceed the customers' comfort level, as described previously in Section 6.1.

This means that the desired load should be within the range of feasible set point changes. If the desired load is outside of this range, the controller will not be able to follow it without causing discomfort to customers, and therefore, it is not a feasible desired demand.

Assuming that the aggregated power can be modeled with a second-order system, the transfer function representation is given by:

$$\frac{Y_s(z)}{U_s(z)} = \frac{b_1 z^{-1} + b_2 z^{-2}}{1 + a_1 z^{-1} + a_2 z^{-2}} \quad (31)$$

Here, $Y(z)$ and $U(z)$ represent the z-transform of the $y_s(k)$ and $u_s(k)$ signals, respectively. This equation in time domain will be:

$$b_1 u_s(k-1) + b_2 u_s(k-2) = y_s(k) + a_1 y_s(k-1) + a_2 y_s(k-2) \quad (32)$$

In this equation, $y_s(k)$ represents the required changes that should be compensated by changing the thermostat set points, and $u_s(k)$ is the control signal which is the change in thermostat set point, issued by the controller to follow $y_s(k)$. It is assumed that the initial conditions are zero, i.e.:

$$u_s(k) = 0 \quad \text{for } k < 0 \quad (33)$$

and

$$\Delta P_d(k) = 0 \quad \text{for } k \leq 0 \quad (34)$$

If we require $y_s(k)$ to track $\Delta P_d(k)$ over the control interval, then it can be shown that the solution for $u_s(k)$ is:

$$u_s(k) = \rho \Delta P_d(k+1) + \sigma \Delta P_d(k) + \tau \Delta P_d(k-1) + \sum_{i=1}^{k-2} ((-b_2/b_1)^{k-1-i} \tau \Delta P_d(i)) \quad (35)$$

where

$$\begin{cases} \rho = \frac{1}{b_1} \\ \sigma = \frac{a_1 b_1 - b_2}{b_1^2} \\ \tau = \frac{a_2 b_1^2 - a_1 b_1 b_2 + b_2^2}{b_1^3} \end{cases} \quad (36)$$

As discussed earlier, a given desired demand is feasible if, for all time steps k , it satisfies the following two conditions:

$$T_s^0 - \alpha \leq u_s(k) \leq T_s^0 + \alpha \quad (37)$$

or:

$$T_s^0 - \alpha \leq \rho \Delta P_d(k+1) + \sigma \Delta P_d(k) + \tau \Delta P_d(k-1) + \sum_{i=1}^{k-2} ((-b_2/b_1)^{k-1-i} \tau \Delta P_d(i)) \leq T_s^0 + \alpha \quad (38)$$

To ensure the feasibility of a desired demand profile, it is essential to verify that it satisfies Equation (38) for all k samples of the profile. However, in order to obtain a general form for feasibility, it may be useful to study the feasibility of specific class of desired demand profiles.

An example class is the trapezoidal shape, where y_s starts from 0 with a constant slope, reaches a maximum value of P_d^{max} and remains constant for k_c samples, then goes back down to 0 with a constant slope.

One approach to studying feasibility is to determine the length of time that $u_s(k)$ can satisfy (37) when ΔP_d is a ramp. This evaluation can be repeated for different values of the ramp rate.

Figure 5 displays two ramp-shaped desired demand profiles and the corresponding control signal u_s . The u_s curve for each profile is computed using Equation (35) until the customers' comfort level is reached at $T_s \pm \alpha$, where $\alpha = 0.5^\circ C$. The plot illustrates that higher ramp slopes require more changes in T_s , causing the system to reach its limit faster. Consequently, the feasibility of profiles with steeper slopes is lower than those with slower rates of change. Figure 10 compares the feasibility intervals of ramp-shaped desired demand profiles with various slopes.

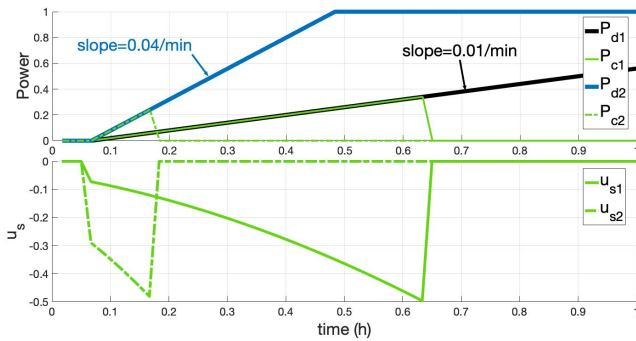


Figure 5: Feasibility intervals for two ramp shape desired demand profiles

It should also be mentioned that the ramp-rate is given for normalized power, which means that the actual rate for power will be obtained by multiplying this rate with the number of individual loads N and nominal power P_{nom} . For instance, a rate of $0.02/min$ for a group of 1,000 air conditioners with a nominal rating of $2kW$ would correspond to a ramp rate of $40kW/min$.

Feasibility studies can also be conducted for the class of trapezoidal-shaped desired demand profiles with varying slope and P_d^{max} . Figure 6 provides an example of such a profile, along with the calculated T_s needed to track the desired demand when α is assumed to be $0.5^\circ C$. As the slope and P_d^{max} values change, so will the corresponding feasibility interval. Figure 12 illustrates how the feasibility interval is affected by these parameters.

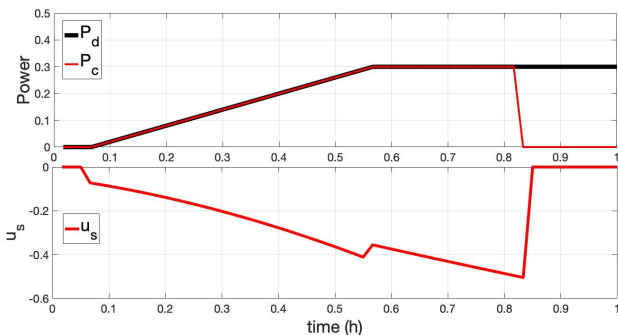


Figure 6: Feasibility interval for a trapezoidal-shaped desired demand

7. Simulation Results

To assess the effectiveness of the proposed method, a numerical simulator was developed in MATLAB to simulate a population of $N = 10,000$ individual air conditioners. As explained in Section 3, we assume that all ACs have the same nominal power, and their thermal capacities follow a log-normal distribution. The simulation employs values listed in Table 1, which have also been used in several other studies.

Table 1: Simulation Parameters [13]

Parameter	Value	Description
P_{nom}	$2kW$	Nominal power rating of the AC
η	3	Coefficient of performance
R	$2^\circ C/kW$	Thermal resistance
μ_C	$3.6kWh/^\circ C$	Mean value of the thermal capacitance
σ_{rel}	0.2	Standard deviation of log-normal distribution for C

7.1. System Modeling

For the given population of ACs in this simulation, the mathematical system that was identified is formulated as:

$$A_a = \begin{bmatrix} 1.975 & -.977 \\ 1 & 0 \end{bmatrix}, B_a = \begin{bmatrix} 1 \\ 0 \end{bmatrix}, C_a = \begin{bmatrix} 0.0027 & -.0025 \end{bmatrix}$$

$$A_s = \begin{bmatrix} 1.898 & -.903 \\ 1 & 0 \end{bmatrix}, B_s = \begin{bmatrix} 1 \\ 0 \end{bmatrix}, C_s = \begin{bmatrix} -.1381, .1376 \end{bmatrix}$$

7.2. Baseline Forecast

Figure 7 shows an example of a forecast profile for the next four hours, generated by the forecasting module at 6:00am on July 3, 2020, using the ambient temperature profile in Barbados. The dashed curve represents the forecasted normalized aggregated power calculated using Equation (16), while the solid curve represents the actual normalized aggregated power calculated using a numerical simulator. The figure illustrates that the forecast module is capable of predicting future power consumption with high accuracy, demonstrating the effectiveness of the mathematical model.

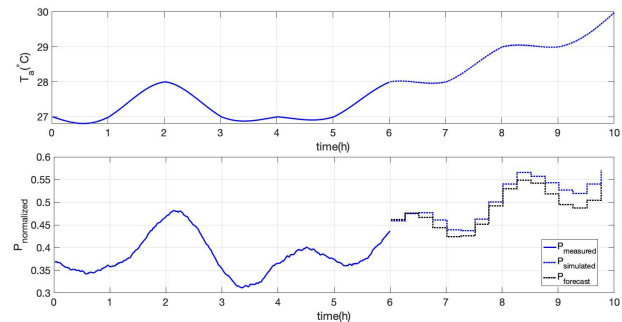


Figure 7: A forecast of the aggregated power consumption, vs. simulated aggregated power consumption in 15 minutes intervals for 4 hours.

Comparison metrics such as the mean absolute percentage error (MAPE), mean absolute error (MAE), and root mean square error (RMSE) are commonly used by researchers to assess the accuracy of forecast models. The proposed method's performance is evaluated using these metrics and compared with other methods in Tables ???. The results show that the proposed method has slightly improved the performance of the baseline forecast. However, the main strength of this method is its ability to predict the load in the presence of control actions, as discussed in the next section. It should also be noted that the MAE and RMSE are calculated based on the normalized power, which is the total power demand divided by the number of loads and the nominal power of each device.

7.3. Forecasting Rebound Effect

Figure 8 illustrates the impact of a desired aggregated load on the original baseline forecast (\hat{P}_b) and the resulting baseline with payback ($\hat{P}_{payback}$). The blue curve represents the original forecast for the baseline load, while the green curve depicts the desired aggregated load. The orange curve shows the resulting forecast after applying the desired load, which includes the payback effect. The payback effect causes the load profile to be higher after the control interval, compared to the profile if no control action was taken. This figure demonstrates how the desired aggregated load can be used to adjust the power consumption profile over a specified interval.

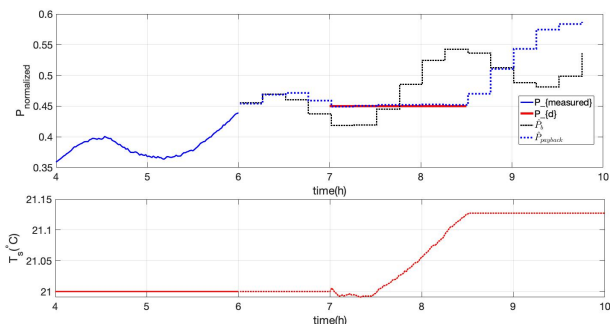


Figure 8: Baseline forecast (\hat{P}_b) and forecast with payback effect ($\hat{P}_{payback}$).

7.4. Forecasting Control Capacity

Figure 9 illustrates an example of using a high-rate slope as a desired demand (the red curve). Applying the mathematical model, the required temperature set point is depicted in green in this figure. Applying these values for the thermostat set points on a simulated population of ACs will result in the aggregated power demand that is shown by the solid blue curve. If we apply a controller to follow this desired demand, the thermostat set point and the aggregated power look like the dotted blue curves.

In Figure 10, the feasibility intervals of desired demand profiles with different slopes are compared. The graph indicates that as the ramp speed increases, the time during which the load can be controlled to align with the desired power consumption decreases. This phenomenon is attributed to the necessity of preserving customers' comfort as discussed earlier.

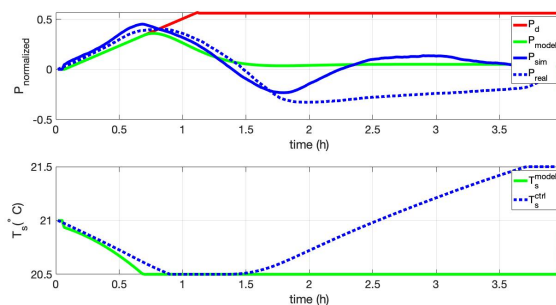


Figure 9: Feasibility of a high-speed ramp desired demand obtained from the model and simulation

Figure 11 illustrates an example of using a trapezoidal-shape as a desired demand (the red curve). Applying the mathematical model, the required temperature set point is depicted in green in this figure. Applying these values for the thermostat set points on a simulated population of ACs will result in the aggregated power demand that is shown by the solid blue curve. If we apply a controller to follow this desired demand, the thermostat set point and the aggregated power look like the dotted blue curves.

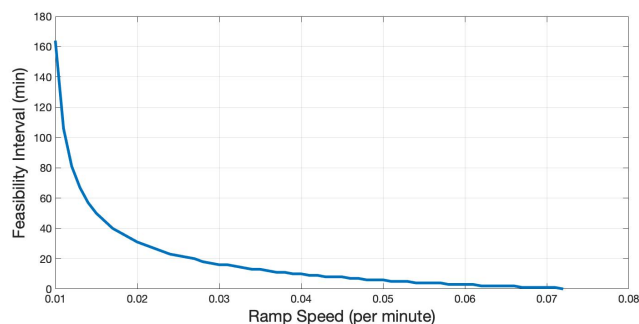


Figure 10: Feasibility intervals for ramp shape desired demand profiles with varying slopes

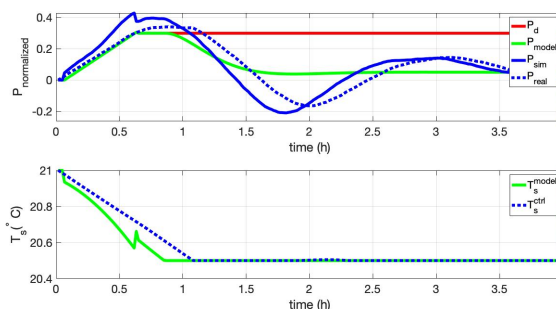


Figure 11: Feasibility of trapezoidal desired demand obtained from the model and simulation

An important aspect of the forecast module is to communicate this information to the system operator. With this knowledge, the operator can make informed decisions on how to generate the desired demand, taking into account the capacity of the controller to track the load.

Figure 12 visually demonstrates the impact on the feasibility interval when altering the slope and P_d^{max} values of the trapezoidal shape. Once more, the observation is evident: a higher slope (faster rate) and a larger maximum value lead to reduced controllability intervals in order to maintain customers' comfort.

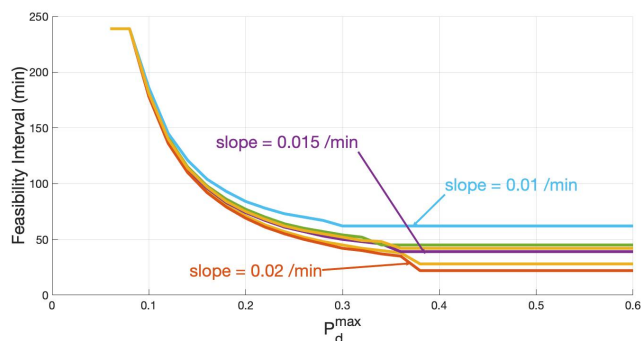


Figure 12: Feasibility intervals for trapezoidal shaped desired demand profiles with varying slopes and P_d^{max}

Conclusions

Thermostatically controlled devices have the potential to be utilized as controllable loads for direct load control, presenting a practical solution to address rapid fluctuations in power generation. The effective management of such loads requires precise predictions of future power consumption and the ability to adjust capacity relative to the baseline.

This study introduces an intelligent agent specifically designed to learn the behavior of a population of air conditioners. It provides a mathematical model for forecasting parameters such as baseline load, controllable load, and the impact of past and present control actions on the forecast. Moreover, the agent assesses potential alterations in the load. The proposed learning mechanism offers two significant advantages: 1) it eliminates the need for knowledge about physical parameters like thermal capacitance or resistance, and 2) it demonstrates adaptability to changing parameters over time. This makes it a practical and versatile plug-and-play load aggregator suitable for deployment in various locations and environments.

References

[1] P. Yazdkhastil, C. P. Diduch, "Smart Agent-Based Direct Load Control of Air Conditioner Populations in Demand Side Management," in 2023 International Conference on Control, Automation and Diagnosis (ICCAD), 1–7, 2023, doi:10.1109/ICCAD57653.2023.10152358.

[2] M. Fan, K. Sun, D. Lane, W. Gu, Z. Li, F. Zhang, "A Novel Generation Rescheduling Algorithm to Improve Power System Reliability with High Renewable Energy Penetration," IEEE Transactions on Power Systems, **33**(3), 3349–3357, 2018, doi:10.1109/TPWRS.2018.2810642.

[3] A. Halder, X. Geng, P. R. Kumar, L. Xie, "Architecture and algorithms for privacy preserving thermal inertial load management by a load serving entity," in 2017 IEEE Power Energy Society General Meeting, 1–1, 2017, doi:10.1109/PESGM.2017.8274310.

[4] Y. Cheng, "Methods for mitigating the effects of intermittent energy production of photovoltaic sources," in 2011 International Conference on Power Engineering, Energy and Electrical Drives, 1–6, 2011, doi:10.1109/PowerEng.2011.6036564.

[5] L. Hucheng, W. Xinwei, Y. Yubo, S. Wei, G. Yanfeng, "Simulation and analysis of electric water heater load regulation model based on direct load control," in 2017 IEEE Conference on Energy Internet and Energy System Integration (EI2), 1–5, 2017, doi:10.1109/EI2.2017.8245591.

[6] M. Shaad, C. P. Diduch, M. E. Kaye, L. Chang, "A basic load following control strategy in a direct load control program," in 2015 IEEE Electrical Power and Energy Conference (EPEC), 339–343, 2015, doi:10.1109/EPEC.2015.7379973.

[7] T. Mega, S. Kitagami, S. Kawawaki, N. Kushiro, "Experimental Evaluation of a Fast Demand Response System for Small/Medium-Scale Office Buildings," in 2017 31st International Conference on Advanced Information Networking and Applications Workshops (WAINA), 291–295, 2017, doi:10.1109/WAINA.2017.84.

[8] M. Shad, A. Momeni, R. Errouissi, C. P. Diduch, M. E. Kaye, L. Chang, "Identification and Estimation for Electric Water Heaters in Direct Load Control Programs," IEEE Transactions on Smart Grid, **8**(2), 947–955, 2017, doi:10.1109/TSG.2015.2492950.

[9] P. Yazdkhasti, C. P. Diduch, "A Mathematical Model for the Aggregated Power Consumptions of Air Conditioners," in 2018 the 6th international conference on smart energy grid engineering, 1 – 8, 2018.

[10] S. Kundu, N. Sinitsyn, S. Backhaus, I. Hiskens, Modeling and control of thermostatically controlled loads, Power Systems Computation Conference, 2011.

[11] W. Zhang, J. Lian, C. Y. Chang, K. Kalsi, "Aggregated Modeling and Control of Air Conditioning Loads for Demand Response," IEEE Transactions on Power Systems, **28**(4), 4655–4664, 2013, doi:10.1109/TPWRS.2013.2266121.

[12] J. Mathieu, S. Koch, D. Callaway, "State estimation and control of electric loads to manage real-time energy imbalance," IEEE Transactions on Power Systems, **28**(1), 430–440, 2013, doi:10.1109/TPWRS.2012.2204074.

[13] N. Mahdavi, J. H. Braslavsky, M. M. Seron, S. R. West, "Model Predictive Control of Distributed Air-Conditioning Loads to Compensate Fluctuations in Solar Power," IEEE Transactions on Smart Grid, **8**(6), 3055–3065, 2017, doi:10.1109/TSG.2017.2717447.

[14] S. H. Tindemans, V. Trovato, G. Strbac, "Decentralized Control of Thermostatic Loads for Flexible Demand Response," IEEE Transactions on Control Systems Technology, **23**(5), 1685–1700, 2015, doi:10.1109/TCST.2014.2381163.

[15] K. Meng, D. Wang, Z. Y. Dong, X. Gao, Y. Zheng, K. P. Wong, "Distributed control of thermostatically controlled loads in distribution network with high penetration of solar PV," CSEE Journal of Power and Energy Systems, **3**(1), 53–62, 2017, doi:10.17775/CSEEJPES.2017.0008.

[16] C.-R. Chen, S.-C. Shih, S.-C. Hu, "Short-term Electricity Forecasting of Air-conditioners of Hospital Using Artificial Neural Networks," in 2005 IEEE/PES Transmission Distribution Conference Exposition: Asia and Pacific, 1–5, 2005, doi:10.1109/TDC.2005.1547136.

[17] D.-X. Niu, Q. Wanq, J.-C. Li, "Short term load forecasting model using support vector machine based on artificial neural network," in 2005 International Conference on Machine Learning and Cybernetics, volume 7, 4260–4265 Vol. 7, 2005, doi:10.1109/ICMLC.2005.1527685.

[18] S. Singh, S. Hussain, M. A. Bazaz, "Short term load forecasting using artificial neural network," in 2017 Fourth International Conference on Image Information Processing (ICIIP), 1–5, 2017, doi:10.1109/ICIIP.2017.8313703.

[19] C. Perfumo, J. H. Braslavsky, J. K. Ward, "Model-Based Estimation of Energy Savings in Load Control Events for Thermostatically Controlled Loads," IEEE Transactions on Smart Grid, **5**(3), 1410–1420, 2014, doi:10.1109/TSG.2014.2298840.

[20] R. Gao, X. Liu, "Short-term load forecasting based on least square support vector machine combined with fuzzy control," in Proceedings of the 10th World Congress on Intelligent Control and Automation, 1048–1051, 2012, doi:10.1109/WCICA.2012.6358034.

- [21] P. Yazdkhasti, C. P. Diduch, "A PID controller for Direct Load Control of Thermostatically Controlled Appliances," in 2019 IEEE 58th Conference on Decision and Control (CDC), 1913–1918, 2019.
- [22] N. Mahdavi, J. H. Braslavsky, C. Perfumo, "Mapping the Effect of Ambient Temperature on the Power Demand of Populations of Air Conditioners," IEEE Transactions on Smart Grid, **9**(3), 1540–1550, 2018, doi: 10.1109/TSG.2016.2592522.
- [23] C. Perfumo, E. Kofman, J. Braslavsky, J. Ward, "Load Management: Model-Based Control of Aggregate Power for Populations of Thermostatically Controlled Loads," Energy Conversion and Management, **55**, 36–48, 2012.
- [24] P. Yazdkhasti, C. P. Diduch, "A Model-Based Short-term Load Forecast Methodology for Aggregated Power Consumption of Thermostatically Controlled Appliances in DSM," in 2021 IEEE Energy Conversion Congress and Exposition (ECCE), 727–732, 2021, doi:10.1109/ECCE47101.2021.9595608.
- [25] L. Von Krannichfeldt, Y. Wang, G. Hug, "Online Ensemble Learning for Load Forecasting," IEEE Transactions on Power Systems, **36**(1), 545–548, 2021, doi:10.1109/TPWRS.2020.3036230.

Copyright: This article is an open access article distributed under the terms and conditions of the Creative Commons Attribution (CC BY-SA) license (<https://creativecommons.org/licenses/by-sa/4.0/>).